

Figure 1: Potential energy profile (including the zero-point energy correction) and geometries of the stationary points for A and B mechanisms, leading to the bidentate double oxygen complex $[\text{ClMg}(\eta^2\text{-O}_2\text{C})]^-$ (**P-A**), and bidentate carbon oxygen complex $[\text{ClMg}(\eta^2\text{-CO}_2)]^-$ (**P-B**) complex. Relative energies (in kcal mol^{-1}) to reactants (**R**).

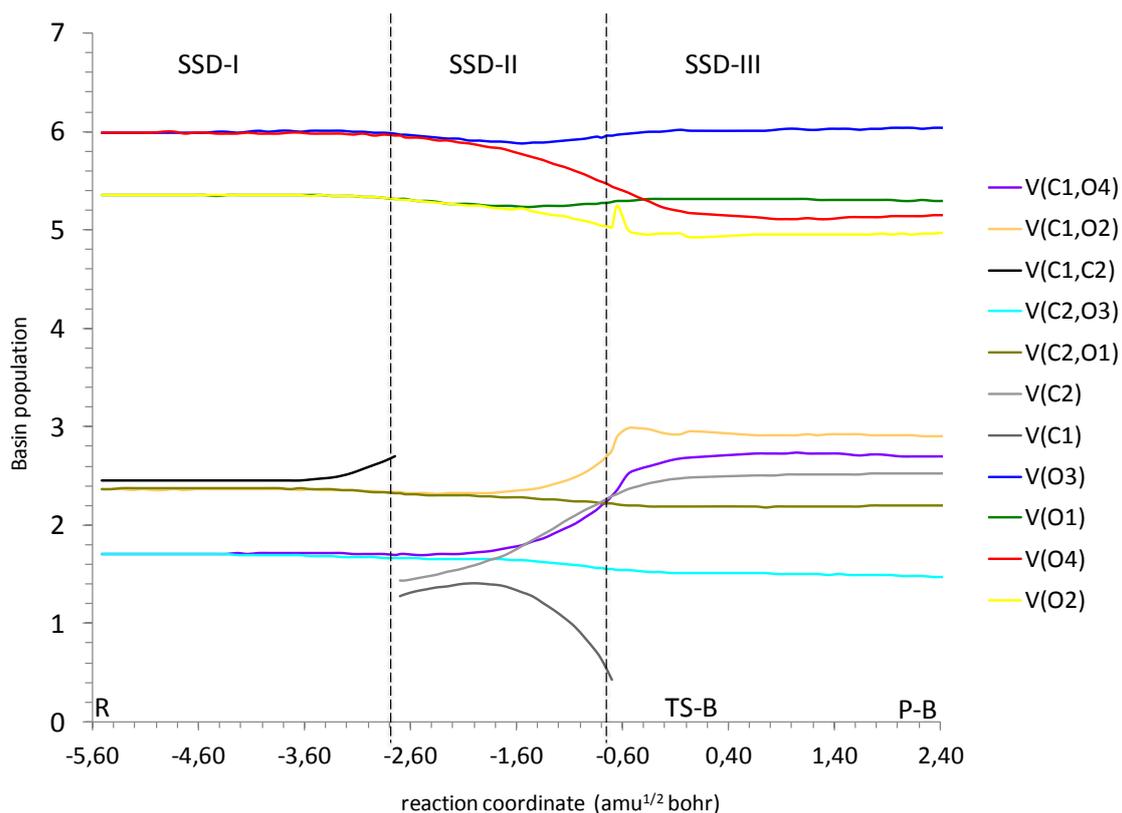


Figure 2. Evolution of the populations of some basins along the IRC pathway for the formation of **P-B** as a function of the reaction coordinate (amu^{1/2} bohr). Dashed lines separate the three structural stability domains (SSD). For the sake of clarity, the valence basin populations of oxygen and chlorine atoms have been unified as a unique basin population, i.e. $V_{i=1,2\dots}(X_i) = V(X_i)$.

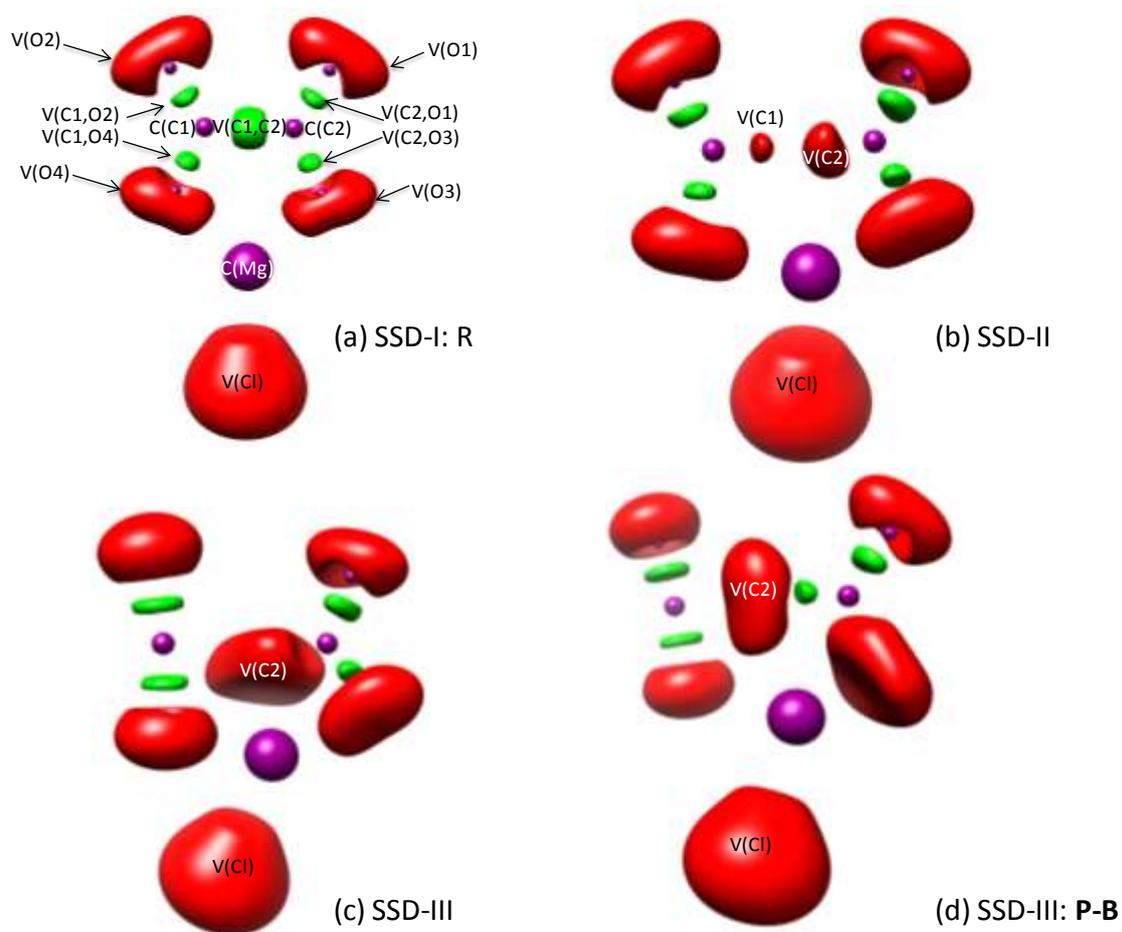


Figure 3. Snapshots of the ELF localization domains for selected points along the IRC for the formation of **P-B**. The isosurface value is $\eta=0.814$. The reaction coordinate value is: (a) $s = -5.519 \text{ amu}^{1/2} \text{ bohr}$ (b) $s = -1.499 \text{ amu}^{1/2} \text{ bohr}$ (c) $s = -0.050 \text{ amu}^{1/2} \text{ bohr}$ (d) $s = 2.591 \text{ amu}^{1/2} \text{ bohr}$. The color code is as follows: green, disynaptic basins; red, monosynaptic basins; purple, core basins.

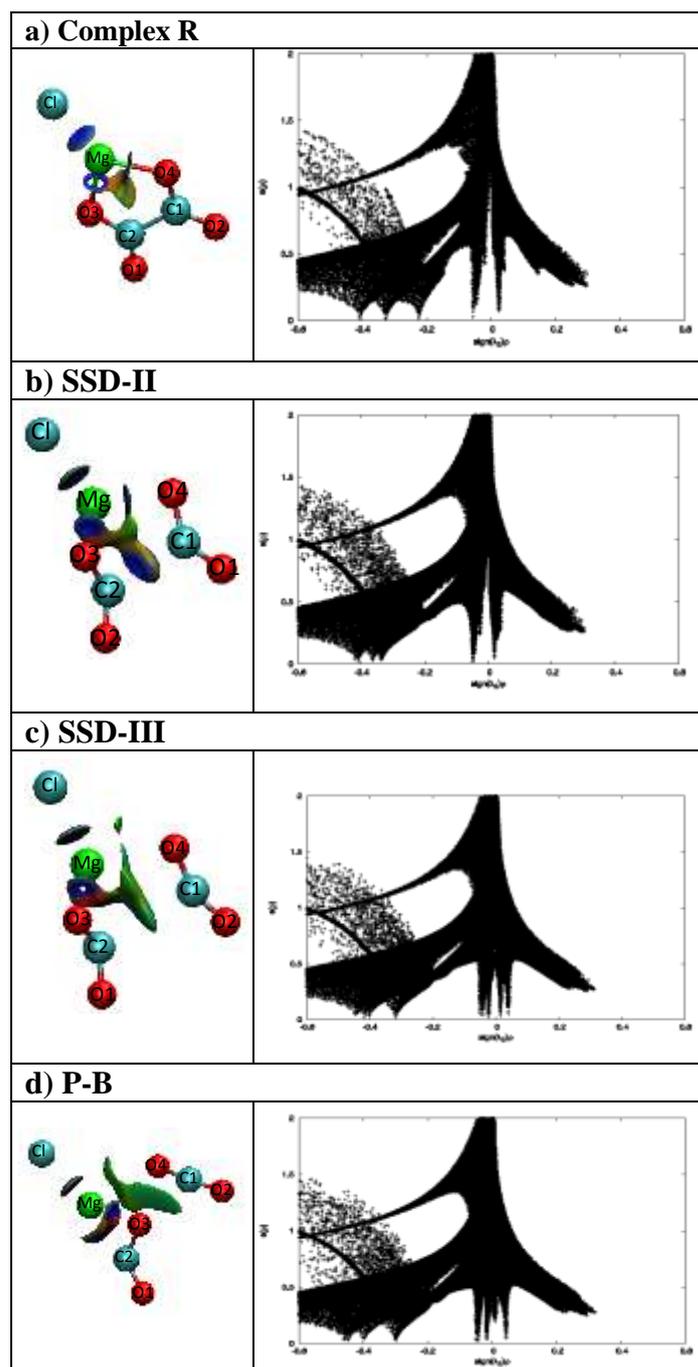


Figure 4. Plots of the reduced density gradient versus the electron density multiplied by the sing of the second Hessian eigenvalue $\rho(r)(\lambda_2)$ and the respective reduced gradient isosurfaces.

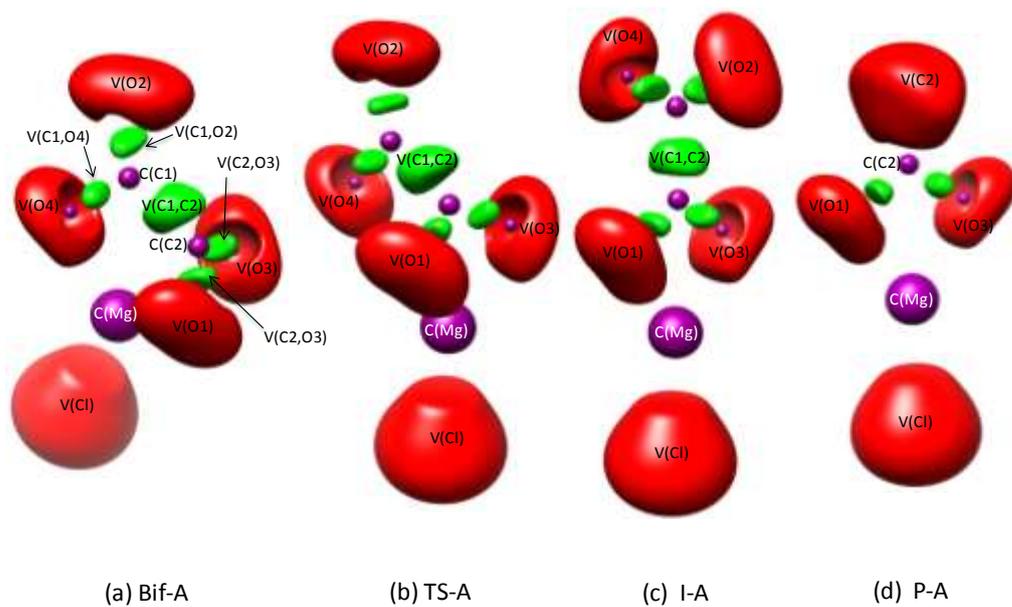


Figure 5. Snapshots of the ELF localization domain ($\eta=0.814$ isosurface) for Bif-A, TS-A, I-A and P-A. The color code is as follows: green, disynaptic basins; red, monosynaptic basins; purple, core basins.